

# Bonding mechanism of Ti/AZ80 dissimilar materials fabricated by spark plasma sintering

Patchara Pripanapong

Graduate School of Engineering

Osaka University

2-1 Yamadaoka, Suita, Osaka, 567-0047, Japan

e-mail address: Patchara@jwri.osaka-u.ac.jp

Junko Umeda, Hisashi Imai, Makoto

Takahashi, Katsuyoshi Kondoh

Joining and Welding Research Institute, Osaka

University

11-1 Mihogaoka, Ibaragi, Osaka, 567-0047, Japan

**Abstract—** In order to reduce a weight of automobile and aerospace component, bonded material between Ti and Mg alloy (AZ80) was fabricated by solid state bonding. Ti and AZ80 could be successfully bonded at bonding temperature and pressure of 400 °C and 40 MPa, respectively. A fine bonding interface was obtained without an existence of crack or void. This is because of high applied pressure which causes a plastic deformation and the formation of high dislocation density areas on Ti and AZ80 side near the bonding interface. The bonded material showed a satisfied bonding strength of 165 MPa which is 78.2% of parent AZ80 alloy. Diffusion of Al element and a formation of Ti<sub>3</sub>Al IMC layer were observed at the bonding interface and considered to be a dominant bonding mechanism.

**Keywords—** Ti; AZ80; solid state bonding; Al diffusion; Ti<sub>3</sub>Al IMC compound

## I. INTRODUCTION

Titanium is a widely applicable material because it possesses many advantages in physical, mechanical and chemical properties. The basic advantage of Ti is high specific strength, which makes Ti suitable to be used for automobile and aerospace components such as valve or connecting rod. The light weight of Ti reduces a fuel consumption and pollution emitted to environment. Titanium is also used for pipe or gas tube in chemical industry because it has a good corrosion resistance. Moreover, a good biocompatibility of Ti makes it suitable to be used in human body such as prosthesis bone or joint [1, 2]. The disadvantage that prevents the widespread applications of Ti is its higher material cost compared to other structural materials such as Mg, Al or steel. It is one of challenge to reduce a cost of component that is fabricated from Ti [3]. Many attempts to reduce a material cost and weight of these Ti components were reported in the previous study [4, 5]. The simple way to reduce a weight of component is to bond Ti with material that possesses lower density such as Al or Al alloys. Many methods have been applied to bond Ti and Al alloys together such as solid state bonding, transient liquid phase bonding, welding and brazing [6-8]. The effective method to join these two materials is solid state bonding because it can prevent a formation of brittle intermetallic compound or heat affected zone (HAZ) [9, 10]. Magnesium as one of structural materials which possesses the lowest density among all of them is also

an interesting material to be bonded to Ti. The difficulty in bonding between Ti and Mg is no intermetallic compounds existing between them in the binary phase diagram [11]. The alloying element in Mg is required in order to form a diffusion layer and IMCs layer with Ti. This result in a capability to bond these two materials with satisfies bonding strength. Atieh et al. tried to bond Ti-6Al-4V and AZ31B (Magnesium alloy) together by transient liquid phase (TLP) bonding, where Ni inserted sheet is applied [12]. However, the bonded material showed low shear strength and brittle fracture surface due to the formation of brittle IMCs layer between Ti-Ni and ternary Mg-Ni-Al in several microns by liquid phase formation. The objective in this study is to bond pure Ti with AZ80 (Mg alloy) by spark plasma sintering (SPS), which is one of the solid state bonding process. The investigation and characterization at the bonding interface were performed including tensile test of the bonded material. This solid state bonding process can control the thickness of IMC layer in nano-level, and result in a high bonding strength between Ti and AZ80.

## II. METHODOLOGY

Pure Ti with purity of 99.95% and AZ80 alloy (Mg-7.8wt%Al-0.3wt%Zn) were used as the bonding materials in order to fabricate a light weight and high strength bonded material. Extruded pure Ti and cast AZ80 rod with 16 mm in diameter were cut to 20 mm height and degreased in acetone. AZ80 was solution treated at 400 °C for 12 hrs in muffle furnace to eliminate the β-Mg (Mg<sub>17</sub>Al<sub>12</sub>) particles which dispersed on Mg matrix, and provide the uniform diffusion of Al in the matrix. Surface of Ti and AZ80 were prepared by grinding with 2000# SiC paper before polishing. The surface of Ti and AZ80 were polished with 0.05 μm alumina colloidal and 0.25 μm diamond pastes, respectively. Surface roughness (R<sub>a</sub>) of both Ti and AZ80 surfaces was measured by a roughness testing machine (ACCRETECH SURFCOM1400G) before bonding from six areas. Microstructure of parent metals (Ti and AZ80) was observed by an optical microscope. Solid state bonding was performed by applying spark plasma sintering machine (SYNTECH CO. SPS103S), where heat and pressure can be simultaneously introduced to sample. Ti and AZ80 rod were inserted into the carbon container, and carbon punches were placed at the end of both side. The temperature was measured by thermocouple which inserted into container wall. The distance from tip of thermocouple to bonding samples was set at 1 mm for

precise measurement. The arrangement of components in SPS chamber and successful bonded sample are shown in fig. 1a and 1b, respectively. Bonding couple were heat to 673 K with heating rate of 20 K/min under vacuum atmosphere of 5 Pa. The pressure of 40 MPa was introduced to bonding couple when starting a bonding process to create a perfect contact between Ti and AZ80 surfaces. Bonding couple were kept at temperature of 673 K for 2 hrs, and cooled in SPS chamber. Interface observation samples were cut from the bonding interface, ground with 2000# SiC paper and polished with 0.25  $\mu\text{m}$  diamond pastes. Microstructure observation at the bonding interface was performed by SEM (JEOL JSM6500F) equipped with energy dispersive spectroscopy (EDS). To investigate a formation of intermetallic compound (IMC) layer, Transmission electron microscope (JEOL JEM-2010) observation was performed at the bonding interface between Ti and AZ80. TEM samples were prepared by focus ion beam machine (HITACHI FB-2000A), where they were sputtered until their thickness was lower than 200 nm. In order to evaluate a bonding strength, three tensile specimens were machined from bonded sample with a diameter and gauge length of 3 and 20 mm, respectively. Tensile test of Ti/AZ80 bonded material was performed at room temperature with testing speed of 0.5 mm/min.

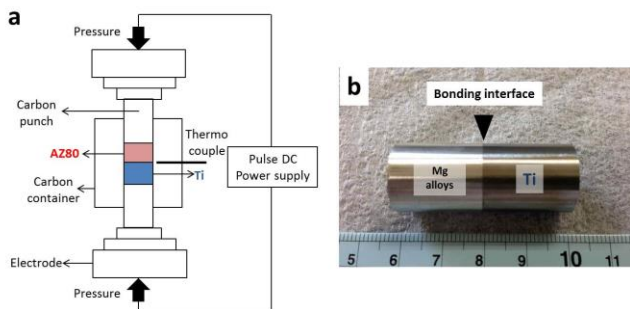


Fig. 1. Schematic drawing of component arrangement inside SPS chamber a) and successful bonded material b).

### III. RESULTS AND DISCUSSION

The roughness ( $R_a$ ) of polished Ti and AZ80 surfaces were measured by a roughness testing machine, where the roughness was measured to be  $0.20 \pm 0.04$  and  $0.15 \pm 0.03$   $\mu\text{m}$ , respectively. The microstructures of Ti and AZ80 after solution treatment are shown in fig. 2. Microstructure of pure Ti showed only  $\alpha$ -Ti matrix, and many of twins (fig. 2a). For AZ80, most of  $\beta$ -Mg particles which generally existed on the matrix were dissolved and the microstructure showed only  $\alpha$ -Mg matrix after solution treatment at 400  $^\circ\text{C}$  for 12 hrs (fig. 2b). The polished surfaces of Ti and AZ80 showed an existence of oxide film with a thickness of 15 nm observed by TEM (fig. 3a and 3b). This oxide film formation is generally occurs on a metal surface when it exposed to oxygen. The existence of oxide film has a disadvantageous effect because it prevents a direct contact between two metal surfaces and inhibits a formation of reaction layer at the bonding interface [13].

Figure 4 shows the bonding interface between Ti and AZ80 after bonding at 400  $^\circ\text{C}$  for 2 hrs under an applied pressure of 40 MPa. The higher density of Ti ( $4.5 \text{ g/cm}^3$ ) was observed in a dark area and the lower density of AZ80 ( $2.8 \text{ g/cm}^3$ ) was observed in a bright area. The TEM image shows that two surfaces are well contacted, and neither crack nor void is observed at the bonding interface. The original oxide film on Ti and AZ80 surface was disappeared after SPS due to the high applied pressure of 40 MPa that caused a plastic deformation of AZ80 on Ti surface, and resulted in a breaking of oxide film [14]. At the same time, the high dislocation density areas were formed near the bonding interface. This area appeared in a dark network on both Ti and AZ80 side [15]. It confirmed that a plastic deformation that contributed to the formation of perfect contact between Ti and AZ80 occurs at the bonding interface.

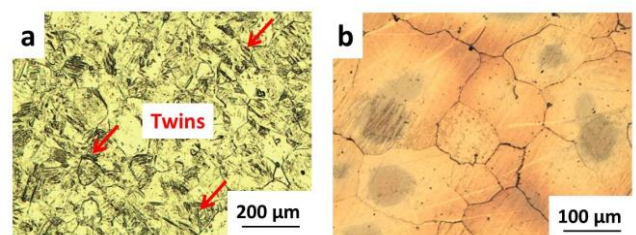


Fig. 2. Optical microstructures of a) Pure Ti and b) Solution treated AZ80 alloy.

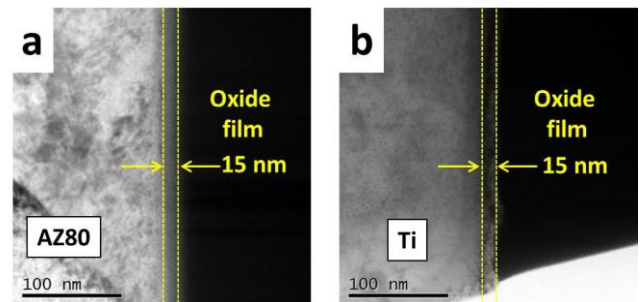


Fig. 3. Existence of oxide film on a) AZ80 alloy surface and b) pure Ti surface observed by TEM.

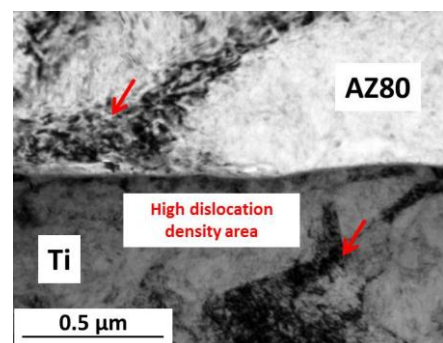


Fig. 4. Bonding interface of Ti/AZ80 after SPS at 400  $^\circ\text{C}$  for 2 hrs under an applied pressure of 40 MPa.

Figure 5 shows a bright field (BF) images and an energy dispersive analysis of Al element at the bonding interface of Ti/AZ80 bonded material. Figure 5a shows a bright field image at the bonding interface, where no intermetallic phase was observed. However, the Al element analysis image (fig. 5b) showed a

diffusion of Al atom from AZ80 to Ti side. This Al concentrated layer has a thickness of about 70 nm. In some area, Al atom diffused, reacted with Ti and formed a short IMC layer of  $Ti_3Al$  with a thickness of 53 nm (fig. 5c). The diffusion of Al and a formation of  $Ti_3Al$  intermetallic layer were considered to be an important mechanism to bond Ti and Mg-Al alloy. Bonding between Ti and Mg is very difficult without a contribution of Al atom according to the binary phase diagram, where no intermetallic compounds exist between them even at high temperatures [11].

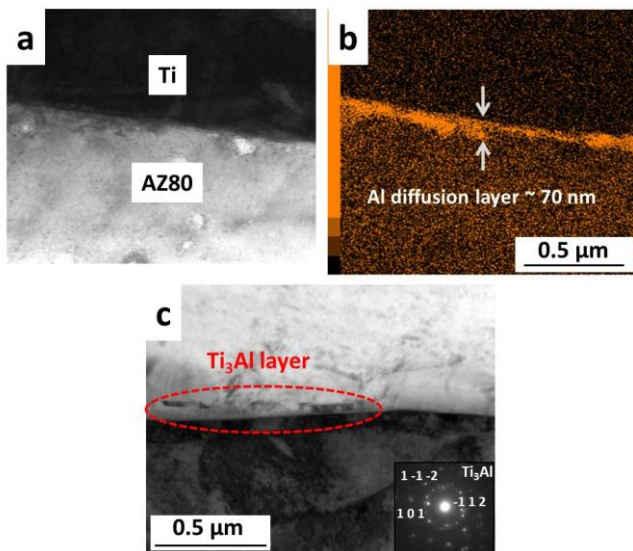


Fig. 5. Bonding interface characterization of Ti/AZ80 bonded material a) BF image, b) Al mapping of a) and c) Formation of  $Ti_3Al$  IMC layer.

Figure 6 shows the tensile Stress-Strain curves of parent metals and Ti/AZ80 bonded material bonded at 400 °C for 2 hrs under an applied pressure of 40 MPa. Tensile strength of Ti, AZ80 and Ti/AZ80 bonded material was 399±5, 212±6 and 163±12 MPa, respectively. The mechanical properties of parent metals and Ti/AZ80 bonded material are listed in table 1. The tensile strength or bonding strength of Ti/AZ80 bonded material was close to tensile strength of AZ80 than that of Ti because the tensile specimens usually fractured on AZ80 side. The bonding efficiency of bonded material was simply calculated from (1) [16]. According to this equation, it suggested that the bonded material shows a satisfied bonding efficiency of 78.2% when compared to tensile strength of parent AZ80 alloy. The elongation of bonded material was similar to elongation of AZ80 than that of Ti but lower in value (0.9±0.2%). This is because a tensile load is concentrates at the bonding interface where elongation and cracks always initially occur on AZ80 side [17]. A young's modulus of bonded material was also similar to parent AZ80 alloy than that of Ti. This is similar to other tensile properties because AZ80 has poorer tensile properties compared to Ti. From these results, the mechanical properties of bonded material seem to depend on the mechanical properties of AZ80 alloy.

$$\text{Bonding efficiency} = (\sigma_b / \sigma_p) \times 100 \quad (1)$$

When,  $\sigma_b$  = Bonding strength of bonding material (MPa)  
 $\sigma_p$  = Tensile strength of parent AZ80 alloy (MPa)

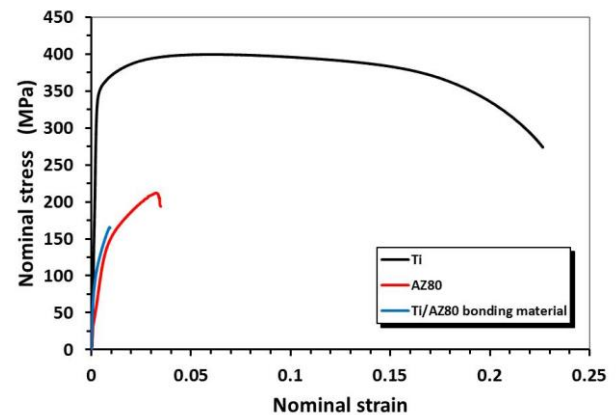


Fig. 6. Tensile Stress-Strain curves of parent metals (pure Ti and AZ80 alloy) and Ti/AZ80 bonded material.

Table 1 Mechanical properties of parent metals and Ti/AZ80 bonded material.

Material	0.2%YS (MPa)	UTS (MPa)	Elongation (%)	Young modulus (GPa)
Pure Ti	355±2	399±5	22.4±1.3	179±25
AZ80 alloy	99±9	212±6	3.5±0.2	47±3
Ti/AZ80	122±12	163±12	0.9±0.2	78±11

Figure 7 shows the fracture surfaces on Ti and AZ80 side after tensile test. Fracture surface observed on AZ80 side showed a severe damage where the material in many areas was gouged out from the surface (fig. 7a). These areas represent an area that exhibited an excellent bonding strength between Ti and AZ80, which even exceeds the strength of parent AZ80 alloy [18]. Accordingly, the large AZ80 debris was found on Ti surface, and the size of debris was comparable to the size of gouged area (fig. 7b). Some of AZ80 debris shows an elongate shape refers to the sliding of AZ80 surface on Ti during SPS. This was an evidence of plastic deformation of AZ80 surface. The fracture surface of Ti showed no damage because the bonding strength of bonded material was much lower than the tensile strength of Ti. The high magnification image of area A showed many of small AZ80 particles attached on the fracture surface of Ti which represented the area that exhibited lower bonding strength compared to the area with a bulk AZ80 debris. This result indicated that a bonding between Ti and AZ80 occurred throughout the bonding surface. The area exhibiting low bonding strength (Ti surface with small AZ80 particles) was attributed to the diffusion of Al atom from AZ80 side to Ti. On the other hand, the area exhibiting high bonding strength (Ti surface with large debris of AZ80) was attributed to a formation of  $Ti_3Al$  IMC layer which was observed in some areas at the bonding interface.

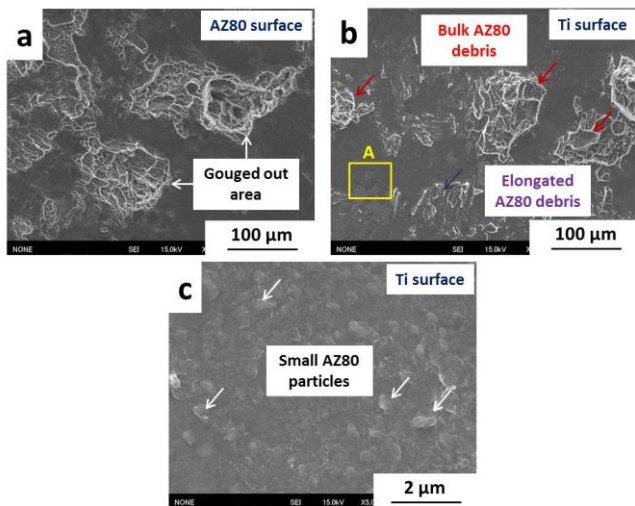


Fig. 7. Fracture surface observation of a) AZ80 surface, b) Ti surface and c) High magnification image of area A in b).

Figure 8 shows the XRD analysis patterns obtained for fracture surface of Ti/AZ80 bonded material bonded at 400 °C for 2 hrs under an applied pressure of 40 MPa on both Ti and AZ80 sides. The x-ray diffraction pattern from AZ80 surface shows the peaks of Mg and Mg<sub>17</sub>Al<sub>12</sub> (β-Mg) which corresponds to the Mg matrix and the small amount of re-precipitated β-Mg after SPS, respectively. There is no Ti peak appeared in the XRD pattern obtained for AZ80 surface which corresponded to SEM image, where no Ti debris was observed on the fracture surface of AZ80. This is explained by the bonding strength of bonded material which is not exceeded the tensile strength of Ti. For Ti side, the peaks of Ti, Mg and Mg<sub>17</sub>Al<sub>12</sub> were observed, which also corresponded to SEM image that many of AZ80 debris were found on fracture surface of Ti. The intensity of Mg peak obtained for fracture surface of Ti was strong because of an existence of large AZ80 debris.

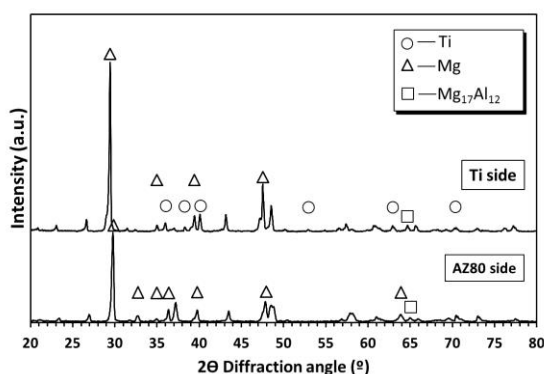


Fig. 8. XRD patterns obtained for fracture surfaces of Ti/AZ80 bonded material bonded at 400 °C for 2 hrs under an applied pressure of 40 MPa.

#### IV. CONCLUSION

Ti and AZ80 are bonded together by the new promising process without applying any inserted sheet for the first time. The following conclusions have been drawn:

1. Ti and AZ80 (Mg-8wt%Al-0.5wt%Zn) are

successfully bonded by spark plasma sintering, which is one of the solid state bonding method. The fine bonding interface without any crack or void is achieved by the effect of plastic deformation on AZ80 surface.

- The diffusion of Al atom from AZ80 side to the bonding interface and the formation of Ti<sub>3</sub>Al IMC layer are dominant mechanism on the bonding between Ti and AZ80. By applying high pressure of 40 MPa, the two bonding surfaces will contact perfectly. This is also one of the important factors in order to achieve a successfully bonding.
- The stress-strain curve of Ti/AZ80 bonded material is similar to the stress-strain curve of parent AZ80 alloy because the tensile specimens usually fracture on the AZ80 side. The fracture surface on AZ80 side shows a severe damage, which is corresponds well to its high bonding strength of 163±12 MPa. The bonded material also shows a high bonding efficiency of 78.2%, which make it become one of very interesting light dissimilar materials.

#### REFERENCES

- [1] L.G. Zhen, L.R. Ze, "Non-aerospace application of Ti materials with a great many social and economic benefits in China," *Mater. Sci. Eng. A.*, 280 (2000) 25-29.
- [2] D. Mareci, R. Chelarui, D.M. Gordin, G. Ungureanu, T. Goriant, "Comparative corrosion study of Ti-Ta alloys for dental applications," *Acta. Biomater.*, 5 (2009) 3625-3639.
- [3] F.H. Froes, H. Friedrich, J. Kiese, D. Bergoint, "Titanium in the family automobile: The cost challenge," *JOM.*, 56 (2004) 40-44.
- [4] Y. Wei, W. Aiping, Z. Guisheng, R. Jialie, "Formation process of the bonding joint in Ti/Al diffusion bonding," *Mater. Sci. Eng. A.*, 480 (2008) 456-463.
- [5] L. Xu, Y.Y. Cui, Y.L. Hao, R. Yang, "Growth of intermetallic layer in multi-laminated Ti/Al diffusion couple," *Mater. Sci. Eng. A.*, 435-436 (2006) 638-647.
- [6] S. Chen, L. Li, Y. Chen, J. Huang, "Joining mechanism of Ti/Al dissimilar alloys during laser welding-brazing process," *J. Alloys. Compd.*, 509 (2011) 891-898.
- [7] X.Y. Nie, J.C. Liu, H.X. Li, Q. Du, J.S. Zhang, L.Z. Zhuang, "An investigation on bonding mechanism and mechanical properties of Al/Ti compound materials prepared by insert moulding," *Mater. Design.*, 63 (2014) 142-150.
- [8] S.P. Gupta, "Intermetallic compound in diffusion couples of Ti with an Al-Si eutectic alloy," *Mater. Charact.*, 49 (2003) 321-330.
- [9] X. Li, W. Liang, X. Zhao, Y. Zhang, X. Fu, F. Liu, "Bonding of Al and Mg with Mg-Al eutectic alloy and its application in aluminum coating on magnesium," *J. Alloys. Compd.*, 471 (2009) 408-411.

[10] G. Mahendran, V. Balasubramanian, T. Senthilvelan, "Developing diffusion bonding windows for joining AZ31B magnesium-AA2024 aluminium alloys," *Mater. Design.*, 30 (2009) 1240–1244.

[11] J.L. Murray, *Bulletin of Alloy Phase Diagrams*, 7 (1986) 245.

[12] Anas M. Atieh, Tahir I. Khan, "Investigating the process parameters on the joint formation of semi-solid TLP bonding of Ti-6Al-4V to Mg-AZ31," *J. Mater. Sci.*, 48 (2013) 6737-6745.

[13] V.Y. Mehr, M.R. Toroghinejad, A. Rezaeian, "The effects of oxide film and annealing treatment on the bond strength of Al-Cu strips in cold roll bonding process," *Mater. Design.*, 53 (2014) 174-181.

[14] A. Miriyev, A. Stern, E. Tuval, S. Kalabukhov, Z. Hooper, N. Frage, "Titanium to steel joining by spark plasma sintering (SPS) technology," *J. Mater. Process. Tech.*, 213 (2013) 161-166.

[15] Y. Lou, L. Li, J. Zhou, L. Na, "Deformation behavior of Mg-8Al magnesium alloy compressed at medium and high temperatures," *Mater. Charact.*, 62 (2011)346-353.

[16] H. Yu, C. Lu, A.K. Tieu, H. Li. A. Godbole, C. Kong, "Annealing effect on microstructure and mechanical properties of Al/Ti/Al laminate sheets," *Mater. Sci. Eng. A.*, 660 (2016) 195-204.

[17] H.R. Akramifard, H. Mirzadeh, M.H. Parzsa, "Estimating interface bonding strength in clad sheets based on tensile test results," *Mater. Design.*, 64 (2014) 307-309.

[18] J. Cao, J. Liu, X. Song, X. Lin, J. Feng, "Diffusion bonding of TiAl intermetallic and Ti<sub>3</sub>AlC<sub>2</sub> ceramic: Interfacial microstructure and joining properties," *Mater. Design.*, 56 (2014) 115-121.